

# Supplementary Material: Modelling the impact of the Omicron BA.5 subvariant in New Zealand

Audrey Lustig, Giorgia Vattiato, Oliver Maclaren,  
Leighton M. Watson, Samik Datta, Michael J. Plank

## Contents

<b>1</b>	<b>Supplementary Methods</b>	<b>2</b>
1.1	Transmission dynamics . . . . .	2
1.2	Vaccination and waning . . . . .	3
1.3	Population dynamics . . . . .	5
1.4	Immunity model . . . . .	7
1.5	Clinical pathways and fitting to data . . . . .	8
	<b>Supplementary Figures</b>	<b>17</b>
1	Number of vaccine doses given over time . . . . .	12
2	Proportion of subvariants in sequenced community cases . . . . .	13
3	Posterior distribution of fitted parameters . . . . .	13
4	Results stratified by immunity status . . . . .	14
5	Age distribution of cases over time . . . . .	15
6	Age-specific case hospitalisation and case fatality ratios . . . . .	15
7	Scenario with small BA.5 growth advantage . . . . .	16
8	Scenario with large BA.5 growth advantage . . . . .	16

# 1 Supplementary Methods

## 1.1 Transmission dynamics

The transmission dynamics are governed by a set of ordinary differential equations for the susceptible ( $S$ ), exposed ( $E$ ), clinical infectious ( $I$ ), subclinical infectious ( $A$ ) and recovered ( $R$ ) compartments for each age group  $i = 1, \dots, n_A$  and susceptibility class  $k = 1, \dots, n_S$ :

$$\frac{dS_{ik}}{dt} = -\lambda_i(1 - e_{I,k})S_{ik} + W_{ik} + G_{ik} \quad (1)$$

$$\frac{dE_{ik}}{dt} = \lambda_i(1 - e_{I,k})S_{ik} - 1/t_E E_{ik} \quad (2)$$

$$\frac{dI_{ik}}{dt} = 1/t_E p_{\text{clin},i}(1 - e_{S,k})E_{ik} - 1/t_I I_{ik} \quad (3)$$

$$\frac{dA_{ik}}{dt} = 1/t_E (1 - p_{\text{clin},i}(1 - e_{S,k})) E_{ik} - 1/t_I A_{ik} \quad (4)$$

$$\frac{dR_{ik}}{dt} = 1/t_I (I_{ik} + A_{ik}) - r_w \hat{r} R_{ik}, \quad (5)$$

where  $t_E$  and  $t_I$  are the latent and infectious periods, respectively,  $p_{\text{clin},i}$  is the probability of testing for a clinical infection,  $r_w$  is the waning rate, and  $\hat{r}$  is the relative rate of moving from recovered ( $R$ ) to susceptible ( $S$ ). For each susceptible compartment, there are associated compartments for people who are: exposed but not yet infectious ( $E$ ); infectious and with clinical symptoms ( $I$ ); infectious and subclinical ( $A$ ); recovered and temporarily immune ( $R$ ). Note that subclinical refers to people who never develop symptoms. For simplicity we do not distinguish between the pre-symptomatic and symptomatic stages of the infectious period for clinical individuals, although it would be straightforward to do this, for example to model symptom-based interventions. Parameter values are shown in Supplementary Tables 1–3.

The  $W_{ik}$  and  $G_{ik}$  terms represent waning and vaccination dynamics (see Sec. 1.2). The force of infection  $\lambda_i$  acting on age group  $i$  is:

$$\lambda_i = \frac{U R_{EI}(t) u_i}{t_I N_i} \sum_{j=1}^{n_A} M_{ji} \left[ \sum_{k=1}^{n_S} (1 - e_{T,k})(I_{jk} + \tau A_{jk}) + t_I n_{\text{seed},j}(t) \right] \quad (6)$$

where  $R_{EI}(t)$  is the time-varying reproduction number excluding effects of immunity,  $N$  is the total population size in each age group,  $n_{\text{seed},j}(t)$  is the number of daily seed infections in age group  $j$  at time  $t$ ,  $\tau$  is the relative infectiousness of subclinical individuals,  $u_i$  is the susceptibility of age group  $i$  relative to the 60-64 year age group, and  $M_{ji}$  is the average number of daily contacts in age group  $i$  by someone in age group  $j$ . The normalising constant  $U$  is set to be

$$U = \rho [(p_{\text{clin},j} + \tau(1 - p_{\text{clin},j})) u_i M_{ji}]^{-1}$$

18 where  $\rho[\cdot]$  denotes dominant eigenvalue. This normalisation ensures that the reproduction  
 19 number at time  $t$  would be  $R_{EI}(t)$  in a fully susceptible population. The contact matrix  $M$   
 20 is based on the results of Prem et al. (2017), adjusted for the New Zealand population by  
 21 Vattiato et al. (2022).

22  $R_{EI}(t)$  represents the value the reproduction number would take if there was no immunity in  
 23 the population, and hence it is unaffected by vaccination, infection and waning dynamics. It  
 24 therefore provides a way to model time-dependence in contact rates, for example as a result  
 25 of behavioural change or policy response.

## 26 1.2 Vaccination and waning

27 As indicated above, the  $G_{ik}$  term in Eq. (1) represents transitions between susceptible  
 28 compartments which occur as a result of vaccination (green arrows in Figure 1). For the  
 29 purposes of calculating this, we define five groups of susceptible compartments  $S^g$ :

$$\text{0 doses and not previously infected:} \quad S_{i0}^g = S_{i1} \quad (7)$$

$$\text{1 dose and not previously infected:} \quad S_{i1}^g = S_{i2} \quad (8)$$

$$\text{2 doses and not previously infected:} \quad S_{i2}^g = \sum_{k=3}^6 S_{ik} \quad (9)$$

$$\geq 3 \text{ doses and not previously infected:} \quad S_{i3}^g = \sum_{k=7}^{10} S_{ik} \quad (10)$$

$$\text{previously infected:} \quad S_{ip}^g = \sum_{k=11}^{14} S_{ik} \quad (11)$$

30 We assumed that all vaccine doses are given to people who are in a susceptible compartment  
 31 (which is reasonable given the recommendation to wait at least 3 months after testing positive  
 32 before getting vaccinated).

33 The total number of people  $V_{id}(t)$  in each age group who have received at least  $d$  doses of  
 34 the vaccine at time  $t$  is:

$$\frac{dV_{id}}{dt} = v_{id}(t) \quad (12)$$

35 where  $v_{id}(t)$  is the number of  $d^{\text{th}}$  doses per day given to people in age group  $i$  at time  $t$ ,  
 36 plus estimated future uptake of fourth doses according to Ministry of Health projections (see  
 37 Figure 1).

38 We assumed that the  $v_{id}$   $d^{\text{th}}$  doses ( $d = 1, 2, 3$ ) given to people in age group  $i$  at time  $t$   
 39 are split pro rata between people who have not been previously infected and people who

40 have. This implies that the daily proportion of those not previously infected in age group  $i$   
 41 receiving their  $d^{\text{th}}$  dose at time  $t$  is

$$p_{i,d}^u = \frac{v_{i,d}}{V_{i,d-1} - V_{i,d}} \quad (13)$$

42 noting that  $V_{i,0} = N_i$ , i.e. the total population size in age group  $i$ . This accounts for  $p_{i,d}^u S_{i,d-1}^g$   
 43 of the  $v_{i,d}$  doses. The remainder of these doses,  $v_{i,d} - p_{i,d}^u S_{i,d-1}^g$ , are given to previously infected  
 44 people. This implies that the daily proportion of those previously infected in age group  $i$   
 45 receiving their  $d^{\text{th}}$  dose at time  $t$  is

$$p_{i,d}^p = v_{i,d} \frac{V_{i,d-1} - V_{i,d} - S_{i,d-1}^g}{(V_{i,d-1} - V_{i,d}) S_{i,p}^g} \quad (14)$$

46 The corresponding equations for 4th or subsequent doses are

$$p_{i,4+}^u = \frac{v_{i,4+}}{V_{i,3}} \quad (15)$$

$$p_{i,4+}^p = v_{i,4+} \frac{V_{i,3} - S_{i,3}^g}{V_{i,3} S_{i,p}^g} \quad (16)$$

47 We may then write the proportion of compartment  $S_{ik}$  receiving a vaccine dose per day as:

$$P_{i,k} = \begin{cases} p_{i,1}^u, & \text{if } k = 1 \\ p_{i,2}^u, & \text{if } k = 2 \\ p_{i,3}^u, & \text{if } 3 \leq k \leq 6 \\ p_{i,4+}^u, & \text{if } 7 \leq k \leq 10 \\ \sum_{d=1}^{4+} p_{i,d}^p, & \text{if } 11 \leq k \leq 14 \end{cases} \quad (17)$$

48 We assume that receiving a vaccine dose following prior infection has the effect of moving  
 49 people back to the first post-infection compartment ( $S_{i,11}$ ) and that receiving a 4th dose with-  
 50 out any prior infection has the effect of moving people back to the first 3-dose compartment  
 51 ( $S_{i,7}$ ).

52 The term  $G_{ik}$  appearing in Eq. (1) is now defined as:

$$G_{ik} = \sum_{l=1}^{n_S} P_{il} S_{il} Q_{lk}^V \quad (18)$$

53 where  $Q_{lk}^V$  is the flux into susceptible compartment  $k$  from susceptible compartment  $l$  as a  
 54 result of vaccine doses given to people in susceptible compartment  $l$ , such that the row sums  
 55 of the matrix  $Q^V$  are all 0.

56 The term  $W_{ik}$  in Eq. (1) represents transitions between susceptible compartments, and  
 57 transitions from recovered to susceptible compartments, that occur as a result of waning  
 58 and is defined as:

$$W_{ik} = r_w \left( \sum_{l=1}^{n_S} S_{il} Q_{lk}^S + \hat{r} \sum_{l=1}^{n_S} R_{il} Q_{lk}^R \right) \quad (19)$$

Parameter	Value
<i>Epidemiological parameters</i>	
Latent period	$t_E = 1$ day
Infectious period	$t_I = 2.3$ days
Mean time from onset of infectiousness to positive test result	$t_T = 4$ days
Mean time from test result to hospital admission	$t_H = 1$ days
Mean time from admission to death	$t_F = 14$ days
Relative infectiousness of subclinical individuals	$\tau = 0.5$
Probability of testing (clinical)	$p_{\text{test,clin}} \sim U[0.35, 0.75]$
Probability of testing (subclinical)	$p_{\text{test,sub}} = 0.4p_{\text{test,clin}}$
<i>Date-specific parameters</i>	
Date of seeding with infectious cases	19 Jan 2022 $+U[-3, 3]$
Number of seed cases in age group $i$	$0.0001N_i$
$R_{EI}(t)$ in period 1	$R_{EI,1} \sim U[2.0, 2.4]$
$R_{EI}(t)$ in period 2	$R_{EI,2} \sim U[2.9, 4.9]$
End of period 1	10 Mar 2022 $+U[-5, 5]$
Period 1 – period 2 ramp window	$U[35, 75]$ days
Relaxation of contact matrix	$\alpha_M \sim U[0, 0.8]$
Contact matrix ramp window	$U[50, 90]$ days
<i>Variant model</i>	
BA.5 immune escape [low,baseline,high]	$r_{VOC} = [0.19, 0.39, 0.59]$
BA.5 change in vaccine-derived log antibody titre relative to BA.2	$\Delta n_{0,VOC} = -0.92$
BA.5 dominance date	$t_{VOC} = 20$ Jun 2022
Variant transition window	$\sigma_{VOC} = 2$ days

Table 1: Model parameter values and prior distributions.

59 where  $Q_{lk}^S$  is the flux into susceptible compartment  $k$  from susceptible compartment  $l$  (with  
60  $Q_{kk}^S \leq 0$  representing the flux out of compartment  $k$ ) such that the row sums of the matrix  $Q^S$   
61 are all 0; and  $Q_{kl}^R \geq 0$  is the flux into susceptible compartment  $k$  from recovered compartment  
62  $l$  such that the row sums of  $Q^R$  are all 1.

### 63 1.3 Population dynamics

64 The dynamics of birth, death and ageing are incorporated into the model via additional  
65 terms in Eqs. (1)–(12) of the form:

$$\frac{dX_{1,k}}{dt} = b - r_a X_{1,k} - \mu_1 X_{1,k} \quad (20)$$

$$\frac{dX_{i,k}}{dt} = r_a (X_{i-1,k} - X_{i,k}) - \mu_i X_{i,k} \quad (21)$$

$$\frac{dX_{n_A,k}}{dt} = r_a X_{n_A-1,k} - \mu_{n_A} X_{n_A,k} \quad (22)$$

Age (yrs)	Popn $N_i(0)$	$u_i$	$p_{clin,i}$	IHR $_i$ per 1000	IFR $_i$ per 1000	$t_{LOS,i}$ (days)	$\mu_i$ (per 1000 per yr)
0-4	305055	0.46	54%	0.94	0.0034	2.0	1.07
5-9	327520	0.46	55%	0.94	0.0034	2.0	0.08
10-14	336975	0.45	58%	0.40	0.0034	2.0	0.17
15-19	316980	0.56	60%	0.60	0.0062	2.0	0.41
20-24	329695	0.79	62%	0.87	0.012	2.0	0.60
25-29	370120	0.93	64%	1.25	0.024	2.0	0.56
30-34	379010	0.97	66%	1.84	0.048	2.7	0.73
35-39	340755	0.98	68%	2.69	0.091	3.3	0.83
40-44	312245	0.94	70%	3.81	0.180	4.0	1.21
45-49	325050	0.93	71%	5.61	0.360	4.7	1.95
50-54	333210	0.94	73%	8.32	0.697	5.4	3.07
55-59	325780	0.97	74%	11.7	1.35	6.0	4.45
60-64	298820	1.00	76%	16.9	2.65	6.7	6.49
65-69	254865	0.98	77%	23.8	5.08	7.4	10.27
70-74	220245	0.90	78%	33.3	9.74	8.0	16.69
75+	346280	0.86	80%	59.7	54.7	8.7	136.0

Table 2: Age-dependent model parameters: ‘Popn’ is the initial population size in each age group;  $u_i$  is the susceptibility of age group  $i$  relative to the 60-64 year age group;  $p_{clin,i}$ , IHR $_i$  and IFR $_i$  are respectively the proportion of infections causing clinical disease, hospitalisation and death respectively for individuals with no immunity (i.e. unvaccinated and no prior infection);  $t_{LOS,i}$  is the average length of hospital stay estimated from MOH data on duration of patients receiving hospital treatment for Covid-19;  $\mu_i$  is the all-cause death rate per 1000 people per year. The age-dependence in IHR $_i$  and IFR $_i$  is based on the results of Herrera-Esposito and de Los Campos (2022) but are scaled down for consistency with New Zealand’s observed hospitalisation and death rates, reflecting a combination of the virulence of Omicron relative to earlier variants and tightening definitions to exclude incidental hospitalisations and deaths. The values of IFR $_i$  the Table are multiplied by a factor  $\alpha_{IFR} \sim U[0.5, 1.5]$  and the values of IHR $_i$  are multiplied by a factor  $\alpha_{IHR} \sim U[0.5, 1.5]$ . Total birth rate  $b = 59637 \text{ yr}^{-1}$ .

66 where  $b$  is the birth rate per unit time,  $r_a$  is ageing rate per unit time (equal to the reciprocal  
67 of the size of the age bands, in this case 5 years) and  $\mu_i$  is the per capita death rate per unit  
68 time in age group  $i$ . Here  $X$  may be any one of the infection states ( $S$ ,  $E$ ,  $I$ ,  $A$ ,  $R$ ) or  $V$ .  
69 For simplicity we assume that the the aggregate population death rate is independent of the  
70 transmission dynamics.

71 The total number of annual births and the annual death rate in 5-year age bands up to age  
72 75 were taken from StatsNZ data for 2019 (StatsNZ, 2022). The annual death rate for the  
73 over-75-years age group was set to give a similar equilibrium age distribution to the StatsNZ  
74 2022 estimated resident population (StatsNZ, 2022).

## 75 1.4 Immunity model

76 We assume immunity for people who are transiently in the one-dose compartment is negli-  
77 gible. Hence  $e_{O1} = e_{O2} = 0$  for all outcomes  $O$ . We set the log antibody titre for susceptible  
78 compartments  $k = 3$  and  $k = 7$  equal to the estimates of Golding and Lydeamore (2022)  
79 for the initial log neutralising titre for 2 doses  $n_{2d,0}$  and 3 doses  $n_{3d,0}$  respectively of the  
80 Pfizer/BioNTech BNT162b2 vaccine against Omicron (see Supplementary Table 3).

81 Following recovery from a first infection, people who have had 3 doses of the vaccine (i.e.  
82 those in recovered compartments  $k = 7, \dots, 10$ ) all move initially to susceptible compartment  
83  $k = 11$ . This is encoded by the matrix  $Q^R$  in Supplementary sec. 1.2:  $Q_{k,11}^R = 1$  for  
84  $k = 7, \dots, 10$ .

85 Following recovery from a first infection, fixed proportions of those in recovered compart-  
86 ments  $k = 3, \dots, 6$  (2 vaccine doses) move to the lower-immunity compartments  $k =$   
87 12, 13, 14. To determine what these proportions should be we note that, absent any sub-  
88 sequent immunising events, the proportion  $q_k(t)$  of a cohort of individuals that entered  
89 susceptible compartment  $k = 11$  at time  $t = 0$  that is in compartment  $k$  at time  $t$  satisfies

$$\dot{q}_k = \begin{cases} -r_w q_k, & k = 11, \\ r_w (q_{k-1} - q_k), & k = 12, 13, \\ r_w q_{k-1}, & k = 14, \end{cases} \quad (23)$$

90 where  $q_{11}(0) = 1$  and  $q_k(0) = 0$  for  $k = 11, 12, 13$ . The average log antibody titre of  
91 the cohort at time  $t$  is  $\bar{n}(t) = \sum_k n_k q_k(t)$ . We set  $Q_{kl}^R = q_l(t^*)$  where  $t^*$  is such that  
92  $\bar{n}(t^*) - \bar{n}(0) = n_{p2d,0} - n_{p3d,0}$ , the estimated difference in initial log titre between prior  
93 infection plus 2 doses and prior infection plus 3 doses according to Golding and Lydeamore  
94 (2022).

95 A similar approach is applied to those moving out of recovered compartments  $k = 1, 2$  (i.e.  
96 people with 0 or 1 vaccine doses following recovery from a first infection): we set  $Q_{kl}^R = q_l(t^*)$   
97 where  $t^*$  is such that  $\bar{n}(t^*) - \bar{n}(0) = n_{p,0} - n_{p3d,0}$ . Following recovery from a second or

Parameter	Value
Initial log antibody titre:	
- 2 doses	$n_{2d,0} = -1.61$
- 3 doses	$n_{3d,0} = -0.92$
- prior infection with 0/1 doses	$n_{p,0} = 1.39$
- prior infection with 2 doses	$n_{p2d,0} = 2.71$
- prior infection with 3 doses	$n_{p3d,0} = 3.56$
Log antibody titre providing 50% immunity:	
- against infection	$n_{\text{inf},50} = -1.61$
- against hospitalisation	$n_{\text{hosp},50} = -3.51$
- against death	$n_{\text{death},50} = -3.51$
Waning rate	$r_w \sim U[0.0027, 0.0063] \text{ day}^{-1}$
Relative rate of moving from $R$ to $S$	$\hat{r} = 1.85$
Drop in log titre in subsequent compartment	$n_{\text{drop}} = 2.30$
Slope of logistic function	$\kappa = 1.28$
Minimum long-term immunity to hospitalisation and death	$e_{\text{sev},\text{min}} = 0.5$

Table 3: Parameters for the immunity submodel. All log titres are given as natural logarithms and represent neutralisation of BA.2. The drop in neutralising titre for BA.5 relative to BA.2 is as described in Methods.

98 subsequent infection, everyone moves initially to susceptible compartment  $k = 11$  regardless  
99 of vaccination status:  $Q_{k,11}^R = 1$  for  $k = 11, \dots, 14$ .

100 To implement the assumptions for an immune escape variant (see Methods), we applied a  
101 time-limited increase in the magnitude of the waning fluxes in Eq. (19) for the post-infection  
102 compartments:

$$W_{ik} = \left( r_w + r_{VOC} \phi \left( \frac{t - t_{VOC}}{\sigma_{VOC}} \right) \right) \left( \sum_{l=1}^{n_S} S_{il} Q_{lk}^S + \hat{r} \sum_{l=1}^{n_S} R_{il} Q_{lk}^R \right), \quad k = 11, 12, 13, 14 \quad (24)$$

103 where  $\phi(\cdot)$  is the standard normal probability density function. This formulation means  
104 that movement of people to a lower post-infection immunity compartment takes place at  
105  $t = t_{VOC}$  in a short time window of duration determined by the parameter  $\sigma_{VOC}$ . In the limit  
106  $\sigma_{VOC} \rightarrow 0$ , this movement occurs as an instantaneous pulse; larger values of  $\sigma$  correspond  
107 to a more gradual change.

## 108 1.5 Clinical pathways and fitting to data

109 The process of testing and progress to different clinical endpoints (hospital admission, hos-  
110 pital discharge, and death) can be modelled downstream of the transmission dynamics. We



111 model the number of newly infectious people in each age group who will eventually become  
 112 a confirmed case ( $C$ ), be hospitalised ( $H$ ), and die ( $F$ ) via the differential equations.

$$\frac{dC_{i1}}{dt} = 1/t_E \sum_{k=1}^{n_S} \left( p_{\text{test,clin}} p_{\text{clin},i} \frac{1 - e_{S,k}}{1 - e_{I,k}} + p_{\text{test,sub}} \left( 1 - p_{\text{clin},i} \frac{1 - e_{S,k}}{1 - e_{I,k}} \right) \right) E_{ik} - \alpha_1 C_{i1} \quad (25)$$

$$\frac{dH_{i1}}{dt} = 1/t_E \text{IHR}_i \sum_{k=1}^{n_S} \frac{1 - e_{H,k}}{1 - e_{I,k}} E_{ik} - \alpha_1 H_{i1} \quad (26)$$

$$\frac{dF_{i1}}{dt} = 1/t_E \text{IFR}_i \sum_{k=1}^{n_S} \frac{1 - e_{F,k}}{1 - e_{I,k}} E_{ik} - \alpha_1 F_{i1} \quad (27)$$

$$(28)$$

113 where  $\text{IHR}_i$  and  $\text{IFR}_i$  are respectively the infection hospitalisation ratio and the infection  
 114 fatality ratio for immune naive individuals in age group  $i$  (see Table 2).

115 The time lag from onset of infectiousness to each endpoint is modelled via transition through  
 116 a series of compartments:

$$\begin{aligned} \frac{dC_{i,2}}{dt} &= \alpha_1 C_{i1} - \alpha_2 C_{i2}, & \frac{dH_{i,2}}{dt} &= \alpha_1 H_{i1} - \alpha_2 H_{i2}, & \frac{dF_{i,2}}{dt} &= \alpha_1 F_{i1} - \alpha_2 F_{i2}, \\ \frac{dC_{i,3}}{dt} &= \alpha_2 C_{i2}, & \frac{dH_{i,3}}{dt} &= \alpha_2 H_{i2} - \alpha_3 H_{i3}, & \frac{dF_{i,3}}{dt} &= \alpha_2 F_{i2} - \alpha_3 F_{i3}, \\ & & \frac{dH_{i,4}}{dt} &= \alpha_3 H_{i3} - \alpha_{4,i} H_{i4}, & \frac{dF_{i,4}}{dt} &= \alpha_3 F_{i3} - \alpha'_4 F_{i4}, \\ & & \frac{dH_{i,5}}{dt} &= \alpha_{4,i} H_{i4}, & \frac{dF_{i,5}}{dt} &= \alpha'_4 F_{i4} - \alpha_5 F_{i5}, \\ & & & & \frac{dF_{i,6}}{dt} &= \alpha_5 F_{i5}. \end{aligned} \quad (29)$$

117 where  $\alpha_k$  are a set of rate constants determining the time lags. We set  $\alpha_1 = \alpha_2 = 2/t_T$  where  
 118  $t_T$  is the mean time from onset of infectiousness to return of a positive test result. The mean  
 119 time from positive test result to hospital admission is  $t_H = \alpha_3^{-1}$ , and the mean length of  
 120 hospital stay for non-fatal cases in age group  $i$  is  $t_{\text{LOS},i} = \alpha_{4,i}^{-1}$ . We set  $\alpha'_4 = \alpha_5 = 2/t_F$  where  
 121  $t_F$  is the mean time from hospital admission to death.

122 The compartment  $C_{i3}$  represents the observed cumulative number of cases,  $H_{i4}$  the number  
 123 of cases currently in hospital,  $H_{i5}$  the cumulative number of hospital discharges and  $F_{i6}$  the  
 124 cumulative number of fatalities in age group  $i$  at time  $t$ . The other  $C$ ,  $H$  and  $F$  variables  
 125 above represent latent (unobservable) states.

126 The variables in Eqs. (29) were used to define a number of key model outputs for model  
 127 fitting and/or comparison with data:

- 128 1. New cases per day:  $\alpha_2 \sum_i C_{i2}(t)$ .
- 129 2. Proportion of new cases in over 60s:  $\sum_{i \geq 13} C_{i2}(t) / \sum_i C_{i2}(t)$ .
- 130 3. New admissions per day:  $\alpha_3 \sum_i H_{i3}(t)$ .

- 131 4. New deaths per day:  $\alpha_5 \sum_i F_{i5}(t)$ .
- 132 5. New infections per day:  $1/t_E \sum_{i,k} E_{ik}(t)/N_i(t)$ .
- 133 6. Hospital occupancy:  $\sum_i H_{i4}(t)$

134 Outputs (1) and (2) were fitted to data from the Ministry of Health on new daily Covid-19  
 135 cases reported from 1 March to 7 July 2022, smoothed using a 7-day rolling average. The  
 136 start date of 1 March was chosen to avoid using data from a period at the start of the first  
 137 Omicron wave when case ascertainment was likely significantly lower due to a lack of testing  
 138 availability.

139 Output (3) was fitted to new daily hospital admissions for Covid-19 from 1 February to 28  
 140 May 2022, smoothed using a 7-day rolling average. The chosen end date ignores the most  
 141 recent 40 days of data to allow for reporting lags. Only hospital admissions categorised by  
 142 the Ministry of Health as “Covid-related hospitalisation” were included – this is significantly  
 143 fewer than the totals reported in the daily updates from the Ministry of Health which include  
 144 all Covid-positive hospital admissions.

145 Output (4) was fitted to daily Covid-19 deaths 1 February to 27 June 2022, smoothed using  
 146 a 7-day rolling average. The chosen end date ignores the most recent 10 days of data to  
 147 allow for reporting lags. Deaths were defined to be cases that were recording as having died  
 148 and where the cause-of-death summary was “COVID as underlying” ( $n = 632$ ), “COVID  
 149 as contributory” ( $n = 355$ ), or “Not available” ( $n = 141$ ) were included; deaths where the  
 150 cause-of-death summary was “Not COVID” ( $n = 332$ ) were excluded.

151 Output (5) was fitted to data on the weekly incidence of new cases in a routinely tested cohort  
 152 of approximately 20,000 border workers from 13 February to 3 July 2022. This may not be  
 153 a representative sample of the population but we include it because, unlike outputs (1–4),  
 154 it provides longitudinal surveillance data that is less sensitive to either case ascertainment  
 155 levels or disease severity.

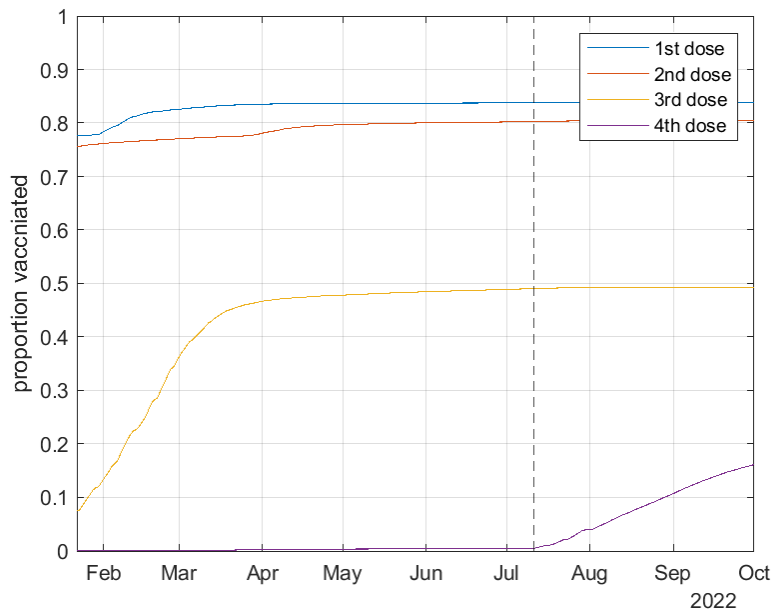
156 We did not fit to output (6) but we compare model output to data on hospital occupancy as a  
 157 key measure of load on the healthcare system. To quantify the number of hospital inpatients  
 158 receiving treatment related to Covid-19 at a given time, we use the hospital admission date,  
 159  $t_a$ , and the Ministry of Health field for the length of hospital stay that is Covid-related,  
 160  $t_h$ . We use this field to assign each hospitalised case a pseudo-discharge date  $t_d = t_a + t_h$ .  
 161 Hospital occupancy at time  $t$  is then defined to be the number of cases with an admission  
 162 date  $t_a \leq t$  and a pseudo-discharge date  $t_d > t$ . This assumes that each inpatient’s period of  
 163 receiving Covid-related treatment is at the start of their hospital stay, which may not always  
 164 be true, but is not expected to have a major effect on results.

165 For each fitted time series (1)–(5), we defined the error function as

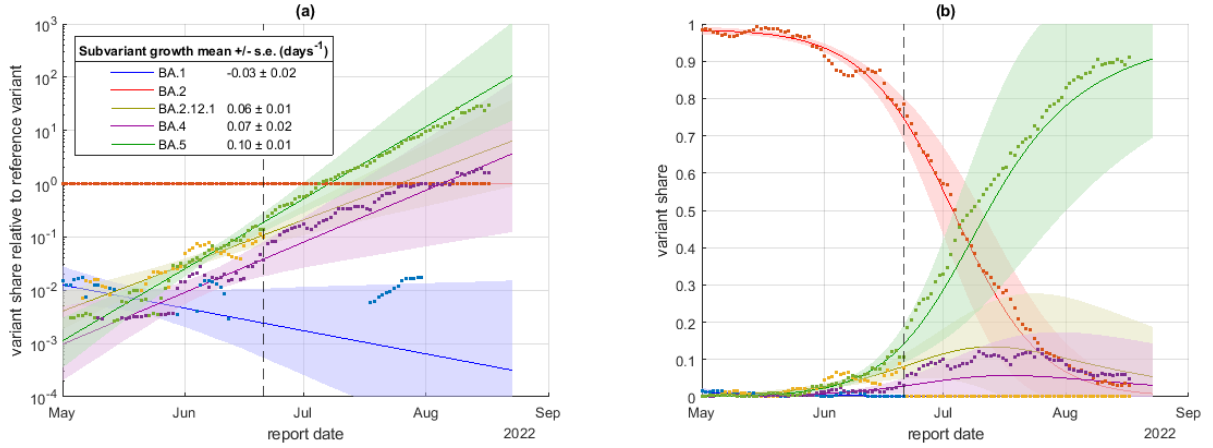
$$d(x, y) = 1/n \sum_{t=1}^n (\ln(x_t + \epsilon) - \ln(y_t + \epsilon))^2, \quad (30)$$

166 where  $\epsilon$  is a fixed value that is small relative to typical values of the variable being fitted:  
167 we set  $\epsilon = 10$  per day for cases,  $\epsilon = 0.5$  for hospital occupancy,  $\epsilon = 0.01$  per day for deaths,  
168  $\epsilon = 5 \times 10^{-5}$  for age distribution of cases, and  $\epsilon = 5 \times 10^{-6}$  per day for incidence per capita.

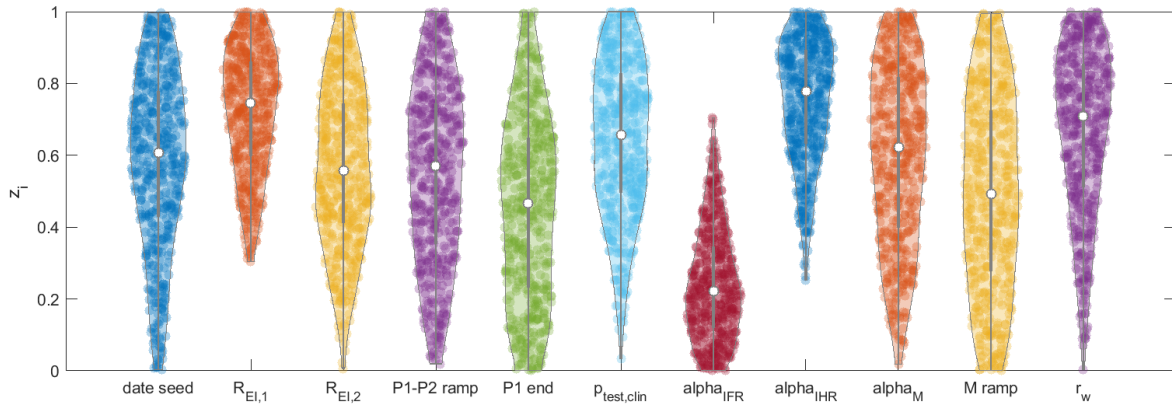
169 The total error is defined as the sum of the error for outputs (1)–(5). To implement ABC  
170 rejection, we solved the model for  $N = 50000$  parameter combinations drawn randomly  
171 from the prior and retained the 500 simulations with the smallest error. We report the  
172 pointwise median and 5th, 25th, 75th and 95th percentiles for each model output across the  
173 500 retained simulations.



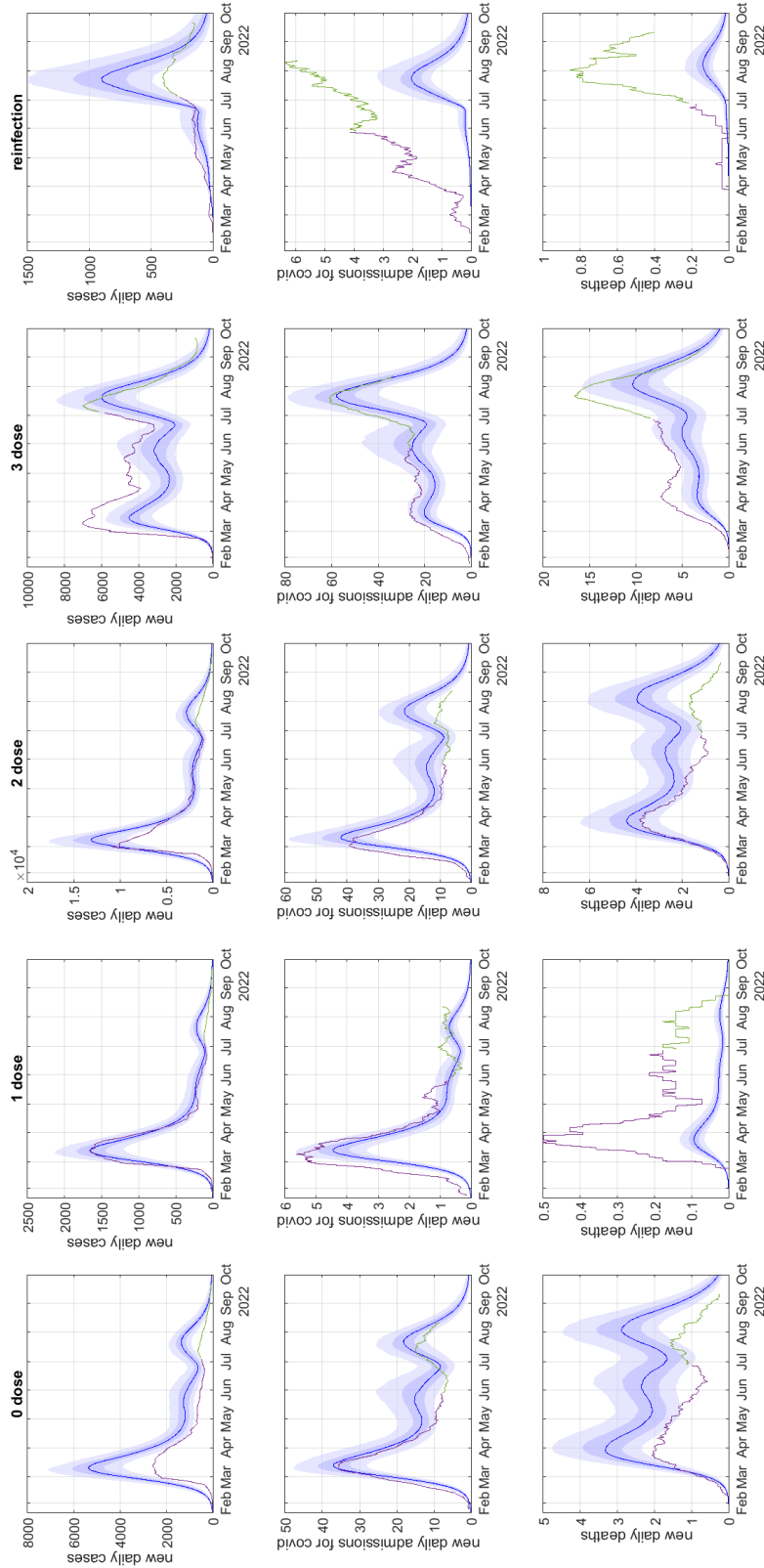
Supplementary Figure 1: Cumulative number of 1st, 2nd, 3rd and 4th doses of the vaccine relative to New Zealand’s population size, based on actual doses administered up to 11 July 2022 (dashed vertical line) and Ministry of Health projections of future uptake of 4th doses after 11 July 2022.



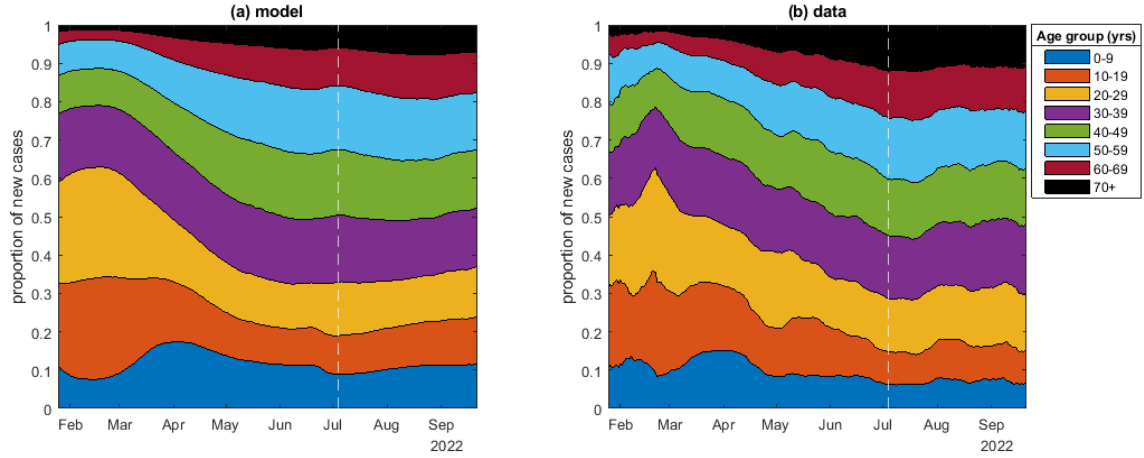
Supplementary Figure 2: Proportion of sequenced community cases that were categorised by ESR (2022) as BA.1, BA.2, BA.2.12.1, BA.4 and BA.5 (points) together with a multinomial regression model (mean and 95% confidence intervals). The model was fitted to data on cases reported up to 21 June 2022 (dashed vertical line), and provides a good prediction of subsequent data. Panel (a) shows the share of each subvariant relative to BA.2, which was the previously dominant variant; (b) shows the absolute share of each subvariant. The multinomial model is equivalent to exponential growth or decay in the ratio of each variant relative to BA.2, which corresponds to straight lines in panel (a). Legend shows the growth rate for each subvariant relative to BA.2 (mean  $\pm$  standard error of the estimated multinomial coefficient). Note: no data is shown for BA.2.12.1 after 21 June 2022 because ESR subsequently stopped reporting the number of BA.2.12.1 sequences.



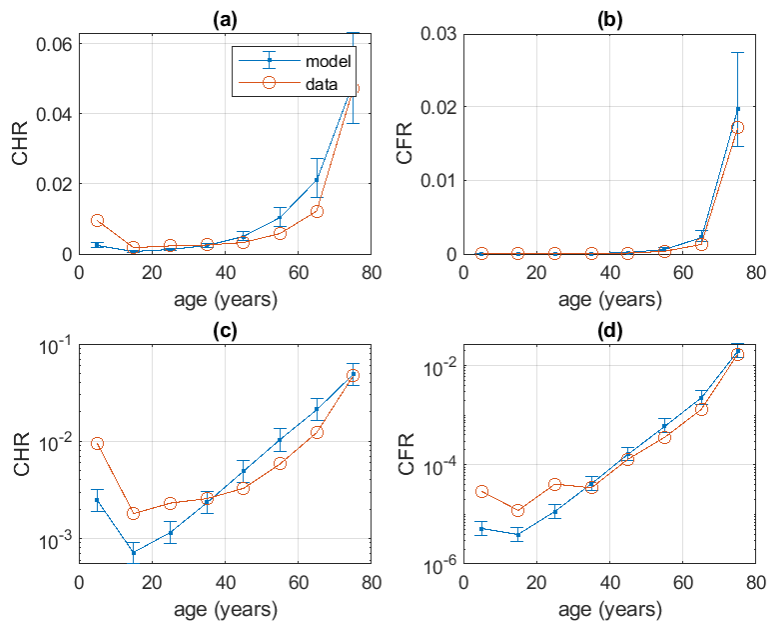
Supplementary Figure 3: Violin plots showing the distribution of each fitted parameter across the 500 accepted realisations of the model with the best fit to the data out of 50,000 random draws from the prior. Each parameter  $\theta_i$  has a uniform prior  $\theta_i \sim U[a_i, b_i]$  (see Tables 1–3) and for the purposes of plotting, each parameter is transformed to the  $[0, 1]$  scale via  $z_i = (\theta_i - a_i)/(b_i - a_i)$ .



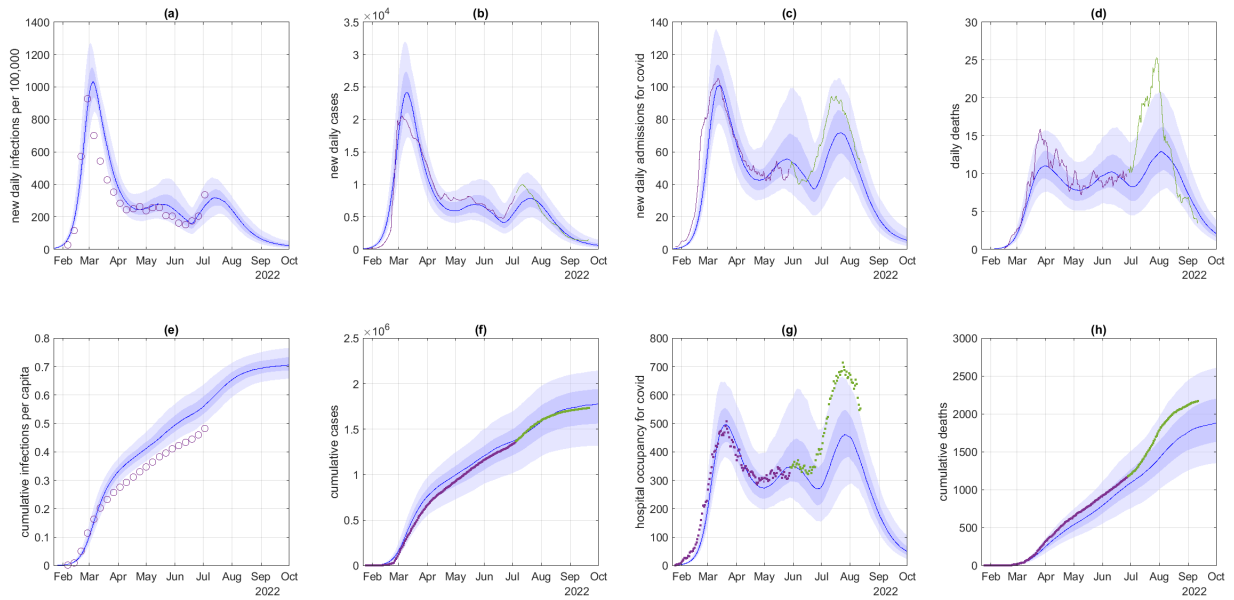
Supplementary Figure 4: Results stratified by immunity status (no prior infections and 0 doses, no prior infections and 1 dose, no prior infections and 2 doses, no prior infection and at least 3 doses, and with prior infection) for the baseline scenario showing new daily cases, new daily hospital admissions and daily deaths. Data on reinfections show individuals with a positive test result reported at least 28 days after a previous positive test results; this definition may include some chronic infections. Model results for reinfections are adjusted for under-ascertainment of the first infection according to the age-specific case ascertainment ratio in the model. Note this assumes that reporting of first infection and subsequent reinfections occur with independently with the same probability, so the comparison should be viewed as approximate. Blue curve shows the median of 500 model simulations and shaded bands show the 5th, 25th, 75th and 95th percentiles. Data (purple curves) show the rolling average over 7 days for cases, 14 days for admissions and 28 days for deaths.



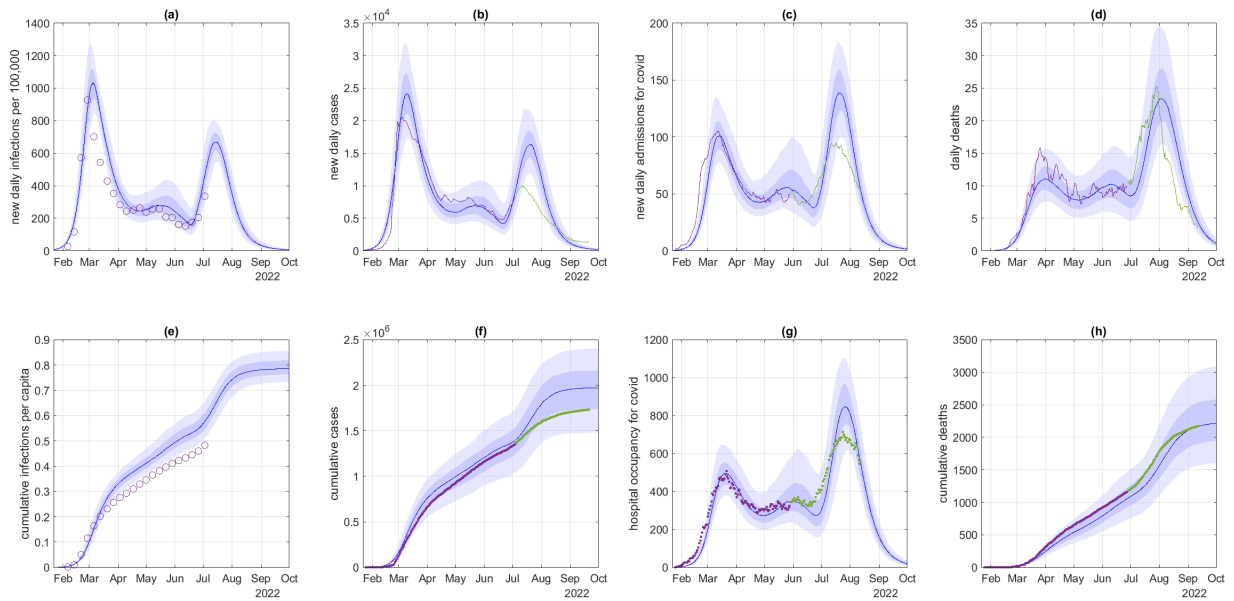
Supplementary Figure 5: Age distribution of new cases in the model compared to the data, shown as the 7-day rolling average. Data before the vertical dotted line at 7 July 2022 was used to fit the model while data afterwards was used for validation.



Supplementary Figure 6: Age-specific case hospitalisation ratio (CHR) and case fatality ratio (CFR). Upper plots show results on a linear scale; lower plots show results on a log scale.



Supplementary Figure 7: As for Figure 3 in the main article but with a smaller growth advantage for BA.5 relative to BA.2 ( $0.07 \text{ day}^{-1}$  instead of  $0.09 \text{ day}^{-1}$ ).



Supplementary Figure 8: As for Figure 3 in the main article but with a larger growth advantage for BA.5 relative to BA.2 ( $0.12 \text{ day}^{-1}$  instead of  $0.09 \text{ day}^{-1}$ ).



## References

- 174
- 175 ESR (2022). Prevelence of SARS-CoV-2 variants of concern in Aotearoa New Zealand.  
176 <https://github.com/ESR-NZ/nz-sars-cov2-variants>.
- 177 Golding, N. and Lydeamore, M. (2022). Analyses to predict the efficacy and waning of  
178 vaccines and previous infection against transmission and clinical outcomes of SARS-CoV-  
179 2 variants. <https://github.com/goldingn/neuts2efficacy>. Accessed 5 April 2022.
- 180 Herrera-Esposito, D. and de Los Campos, G. (2022). Age-specific rate of severe and crit-  
181 ical SARS-CoV-2 infections estimated with multi-country seroprevalence studies. *BMC*  
182 *Infectious Diseases*, 22(1):1–14.
- 183 Prem, K., Cook, A. R., and Jit, M. (2017). Projecting social contact matrices in 152  
184 countries using contact surveys and demographic data. *PLoS Computational Biology*,  
185 13(9):e1005697.
- 186 StatsNZ (2022). Infoshare. <https://infoshare.stats.govt.nz>. Accessed 29 May 2022.
- 187 Vattiato, G., Maclaren, O., Lustig, A., Binny, R. N., Hendy, S. C., and Plank, M. J. (2022).  
188 An assessment of the potential impact of the Omicron variant of SARS-CoV-2 in Aotearoa  
189 New Zealand. *Infectious Disease Modelling*, 7:94–105.